

# Link and System Level Performance of Multiuser Detection CDMA Uplink

Antti Toskala, Seppo Hämäläinen and Harri Holma

*Nokia Research Center, P.O. Box 407, FIN-00045 NOKIA GROUP, Finland. E-mail:*

*antti.toskala@research.nokia.com, seppo.hämäläinen@research.nokia.com &*

*harri.holma@research.nokia.com*

## Abstract

The link level performance and the cellular system capacity in the uplink direction of a CDMA cellular system utilising multiuser detection base station receivers is analysed by simulation. In the receiver, parallel multistage multiuser detection is employed together with two-antenna diversity reception and fast closed-loop power control. A system level simulator is built to utilise the link level simulation results and to show the increase in cellular capacity obtained by using multiuser detection. The capacity is studied in urban micro and macro-cell environments utilising the channel models developed in the European CODIT project. The modelling of the environment specific and CDMA specific features is considered in the system simulator. The system level simulator is calibrated with analytical capacity calculations.

## 1. INTRODUCTION

Third generation mobile communication systems have been under intensive study and development recently. One candidate for the air interface is DS-CDMA which is currently being used for the second generation cellular systems. The current CDMA technology, however, has shortcomings that prevent it from achieving the full potential of the technology and meeting the high demands of the air interface of the third generation systems. The motivation to study DS-CDMA for the third generation mobile communication systems is the potential to offer good flexibility in the introduction of new services and allowing a mix of different data rates.

In this paper the link level performance and cellular capacity of DS-CDMA with multistage Multiuser Detection (MUD) is considered in an asynchronous uplink. The MUD algorithm is based on nonlinear parallel interference cancellation and has been introduced in [1-3]. The performance of this receiver has been evaluated by simulations in a multipath fading channel in [4]. The link level simulations include antenna diversity and fast closed loop power control. The uplink multirate concept with a mix of different data rates with MUD has been studied in [5]. Other approaches to the interference cancellation have been studied in the link level in several publications, for the linear decorrelating approach for example in [6] and for the nonlinear regenerating type multistage in [7]. Also adaptive detectors have been proposed for the cases when there is no knowledge on the interference parameters, as in [8-9]. The channel models applied in the simulations are obtained from the European RACE project R2020 Code Division Testbed (CODIT) [9]. In order to reduce the complexity of the receiver

the number of RAKE fingers is limited, i.e. only part of the energy is captured in simulations.

The evaluation of cellular capacity is based on a system level simulator. Instead of relying only on analytical formulas we also resort to a simulator based approach in order to model the effect of multiuser detection correctly. A semi-static approach is chosen for the network simulator to address CDMA specific features such as fast power control.

The performance is analysed for the uplink only, as in the uplink reception all the users are to be detected anyway and less complexity restrictions apply when compared to the downlink terminal reception. Additionally in the downlink transmission orthogonal or near-orthogonal codes can be used. The multistage algorithm studied has been chosen since it does not require any computationally complex operations, such as correlation matrix inversions or factorizations. Neither is chip level regeneration needed.

This paper is organised as follows. General descriptions of the link level and system level are given in Section 2. CODIT channel models are introduced in Section 3. In Section 4 the multistage MUD algorithm with antenna diversity and SIR based power control is presented. Link level simulation parameters and simulation results are shown in Section 5. The semi-static system level simulation principles are presented in Section 6 and cellular capacities with and without MUD in micro and macro-cellular environments in Section 7. Finally, conclusions are presented in Section 8.

## 2. SYSTEM DESCRIPTION

An uplink is considered with  $K$  asynchronous CDMA transmitters transmitting in a common frequency band. Each user is assigned a spreading waveform given by

$$s_k(t) = \sum_{m=1}^N S_k^m \prod_{T_c} (t - mT_c) \quad (1)$$

where  $\prod_{T_c}$  is a rectangular impulse of the chip length  $T_c$ . The  $m$ th chip of the  $k$ th user's spreading sequence is given as

$$S_k^m \in \{-1, 1\}, k = 1, \dots, K \quad (2)$$

The waveform is now time limited to  $[0, T)$  where  $T$  is the symbol length. The spreading waveforms are modulated with BPSK symbols  $b_k^{(i)} \in \{-1, 1\}$ . The baseband form of the received signal at the base station receiver is now given by

$$r(t) = \sum_{i=-P}^P \sum_{k=1}^K h_k(t) * b_k^{(i)} \sqrt{\frac{E_k}{T}} s_k(t - iT) + n(t) \quad (3)$$

where  $2P+1$  is the length of a data packet,  $E_k$  is the transmitter energy for user  $k$  and  $n(t)$  represents baseband white Gaussian noise with two-sided power spectral density with height  $N_0/2$ . Gaussian noise represents here thermal noise plus interference from neighbouring cells. The symbol  $*$  denotes convolution and  $h_k(t)$  is the  $k$ th user's impulse response of the multipath channel, given as

$$h_k(t) = \sum_{l=1}^{L'} h_{k,l}(t) \delta(t - \tau_{k,l}(t)) \quad (4)$$

where  $h_{k,l}$  is the complex channel tap for the  $k$ th user's  $l$ th propagation path and  $L'$  is the number of paths associated with the channel. In the simulations,  $L'$  is assumed to be finite and it is determined by the used channel model. However, due to a finite bandwidth, the receiver will not be able to resolve all  $L'$  paths. Propagation delays  $\tau_{k,l}(t)$  are assumed to be known *a priori* or obtained from a delay estimator and they remain unchanged during the transmission. Omitting the time index we write the different delays as  $\tau_{k,l}$ . The complex channel taps are determined by the channel model described in Section 3.

### 3. CODIT CHANNEL MODELS

In the simulations we have applied an urban macro-cell channel model and an urban street micro-cell channel model developed in the European CODIT project [9]. The urban macro-cell transmission environment is composed of the base station positioned at a high elevation and the mobile station surrounded by a very dense irregular scattering structure with no line-of-sight. The channel model consists of 20 scatterers each having a Rayleigh fading character. The delay spread is

2.0  $\mu$ s. The chip length in simulations is 0.195  $\mu$ s resulting in 11 resolvable paths. An example sequence of delay profiles in macro-cell at 50 km/h is shown in Fig. 1.

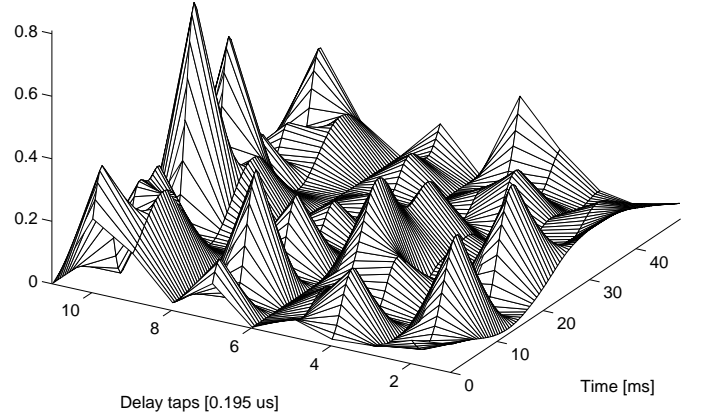


Fig. 1. Delay profiles in the simulated CODIT urban macro-cell

The urban street micro-cell is a linear street flanked on both sides by a dense distribution of buildings and intersected by side streets. The base station antenna is located below the building height. The delay profile consists of a strong first arriving path, 4 further paths within 50 ns, local scattering within 100 ns and further weaker paths up to 1.8  $\mu$ s. More than 90 % of the energy is within 0.1  $\mu$ s. With the chip length of 0.195  $\mu$ s this micro-cell channel model is close to a single path channel.

Both the channel models have constant delays, i.e. path delays remain the same during a simulation run.

### 4. MULTISTAGE MULTIUSER DETECTOR

In our base station receiver front-end the received signal  $r(t)$  is despread using the known delays and spreading waveforms as

$$z_{k,l}^{(i)} = \int_{iT + \tau_{k,l}}^{(i+1)T + \tau_{k,l}} r(t) s_k^*(t - \tau_{k,l} - iT) dt \quad (5)$$

with  $T$  indicating here the symbol length. The matched filter outputs are collected in a vector

$$\mathbf{z}_k^{(i)} = \left( z_{k,1}^{(i)}, \dots, z_{k,L}^{(i)} \right) \quad (6)$$

where  $L$  is the number of RAKE fingers per user. These vectors are further collected in one vector for all  $K$  users as

$$\mathbf{z}^{(i)} = \left( \mathbf{z}_1^{(i)}, \dots, \mathbf{z}_K^{(i)} \right) \quad (7)$$

The sequence of matched filter outputs from the receiver front-end is given as

$$\mathbf{z} = (\mathbf{z}^{(-P)}, \dots, \mathbf{z}^{(P)})^T \quad (8)$$

over the whole packet length. The amplitudes are assumed to be constant during one symbol interval, and the amplitude is defined as

$$\alpha_{k,l}(t) \equiv \sqrt{\frac{E_k}{T}} h_{k,l}(t) \quad (9)$$

with the complex amplitude for the  $i$ th symbol of the  $k$ th user's  $l$ th path given now as  $\alpha_{k,l}^{(i)}$  and for a single symbol interval as

$$\mathbf{a}_k^{(i)} = (\alpha_{k,1}^{(i)}, \dots, \alpha_{k,L}^{(i)}) \quad (10)$$

and the matrix containing the received amplitudes for all users is denoted by

$$\mathbf{A}^{(i)} = \text{diag}(\mathbf{a}_1^{(i)}, \dots, \mathbf{a}_K^{(i)}) \quad (11)$$

The multistage multiuser detection requires a knowledge of the correlations between users' propagation paths in order to cancel the interference. This correlation matrix can be calculated from the users' delays and from their spreading waveforms. We assume here that the diversity antennas are close enough to each other that the delays  $\tau_{k,l}$  are the same for both antenna branches. A single matrix element denoting the correlation between the  $k$ th user's  $l$ th propagation path and the  $k'$ th user's  $l'$ th path can be given as

$$\left[ \mathbf{R}_{k,k'}^{(n)} \right]_{l,l'} = \int_{-\infty}^{\infty} s_k(t - \tau_{k,l}) s_{k'}^*(t - \tau_{k',l'} + nT) dt \quad (12)$$

To simplify the notation we define also the following matrices, given as

$$\mathbf{R}^{(n)} = \begin{pmatrix} \mathbf{R}_{1,1}^{(n)} & \dots & \mathbf{R}_{1,K}^{(n)} \\ \vdots & \ddots & \vdots \\ \mathbf{R}_{K,1}^{(n)} & \dots & \mathbf{R}_{K,K}^{(n)} \end{pmatrix} \quad (13)$$

$$\mathbf{R}_N = \begin{pmatrix} \mathbf{R}^{(0)} & \dots & \mathbf{R}^{(2N)} \\ \vdots & \ddots & \vdots \\ \mathbf{R}^{(-2N)} & \dots & \mathbf{R}^{(0)} \end{pmatrix} \quad (14)$$

The matrix  $\mathbf{R}_N$  contains the correlations affecting the despread signal over  $N$  neighbouring symbol intervals. The size of the matrix depends on the maximum delay spread and on the symbol length. The matched filter outputs are now given as

$$\mathbf{z} = \mathbf{R} \mathbf{A} \mathbf{b} + \mathbf{n} \quad (15)$$

with  $\mathbf{A}$  given as

$$\mathbf{A} = \text{diag}(\mathbf{A}^{(-P)}, \dots, \mathbf{A}^{(P)}) \quad (16)$$

and  $\mathbf{b}$  as

$$\mathbf{b} = (\mathbf{b}^{(-P)}, \dots, \mathbf{b}^{(P)})^T \quad (17)$$

where

$$\mathbf{b}^{(i)} = (b_1^{(i)} \mathbf{1}_L^T, \dots, b_K^{(i)} \mathbf{1}_L^T) \quad (18)$$

with  $\mathbf{1}_L = (1, \dots, 1)^T$  a vector of length  $L$ .

The optimum solution [10] for multiuser detection is difficult to implement since the complexity increases exponentially as a function of the number of users  $K$  and the number of RAKE fingers per user  $L$ ; therefore less complex suboptimum solutions have to be studied. The solution under study in this paper is the multistage detector given originally in [1] and [2] and for multipath channels in [3]. The problem formulation is given in [4]. The receiver can be expressed as

$$\hat{\mathbf{b}}(m+1) = \text{sgn}[\bar{\mathbf{A}}_a \mathbf{z}'] \quad (19)$$

where

$$\mathbf{z}' = \mathbf{z} - (\mathbf{R} - \mathbf{I}) \hat{\mathbf{A}} \hat{\mathbf{b}}(m) \quad (20)$$

and  $m$  is the stage and

$$\bar{\mathbf{A}}_a = (\mathbf{I}_{K(2P+1)} \otimes \mathbf{1}_L^T) \hat{\mathbf{A}}_a^* \quad (21)$$

describes the maximal ratio combining at the decision stage.

Here  $\otimes$  denotes the Kronecker product. In (21)  $\hat{\mathbf{A}}_a$  is the estimate of  $\mathbf{A}$  in (16). The index  $a$  separates different antenna elements. The conventional receiver can be simply described as

$$\hat{\mathbf{b}}_{\text{RAKE}} = \text{sgn}[\bar{\mathbf{A}}_a \mathbf{z}] \quad (22)$$

The used power control is based on the signal-to-interference ratio (SIR) with SIR estimated from the 'cleaned' matched filter outputs  $\mathbf{z}'$ . The power control of the conventional RAKE receiver is based on matched filter outputs  $\mathbf{z}$ .

The channel coefficients are estimated with sequential multiuser channel estimation utilising the symbol decisions as

$$\begin{aligned} \hat{\mathbf{A}}_a^{(i+1)} &= \hat{\mathbf{A}}_a^{(i)} + \gamma_1 (\hat{\mathbf{A}}_a^{(i)} - \hat{\mathbf{A}}_a^{(i-1)}) \\ &+ \gamma_2 \hat{\mathbf{B}}^{(i)} \text{diag}(\mathbf{z}_a^{(i)} - \mathbf{R} \hat{\mathbf{A}}_a^{(i)} \hat{\mathbf{b}}^{(i)}) \end{aligned} \quad (23)$$

where

$$\mathbf{B}^{(i)} = \text{diag}(\mathbf{b}_1^{(i)}, \dots, \mathbf{b}_K^{(i)}) \quad (24)$$

and the suitable values for the parameters  $\gamma_1$  and  $\gamma_2$  depend mainly on the mobile speed and on the propagation

environment. The corresponding conventional channel estimator neglects the correlation information.

The multiuser detection base station receiver with antenna diversity and closed loop power control is shown in Fig. 2. Matched filters are used as a pre-stage to obtain the initial symbol estimates.

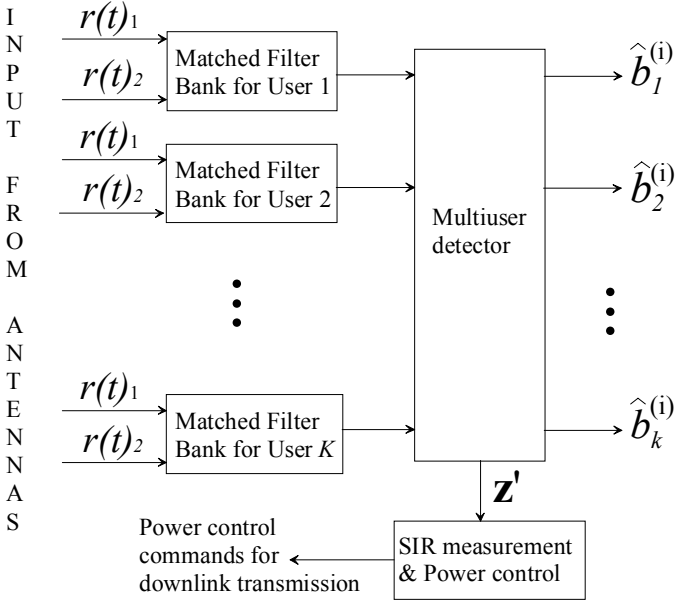


Fig. 2. Multiuser receiver with antenna diversity

## 5. LINK LEVEL SIMULATIONS

The bit error rate (BER) performances in Monte Carlo simulations are used to assess the efficiency  $\beta$  of multiuser detection. This efficiency denotes the percentage of intra-cell interference being removed by multiuser detection at the base station receiver. The efficiency of MUD is estimated from the load that can be accommodated with a specific  $E_b/N_0$  value with a conventional RAKE receiver and with a multiuser receiver. The additive white Gaussian noise  $N_0$  is used to represent both thermal noise and interference from neighbouring cells while intra-cell interference is represented by actual signals. The  $E_b/N_0$  values have been chosen according to the estimated maximum cellular capacity. The target BER is  $10^{-3}$ . In the analysis, we denote the number of users with a RAKE receiver by  $K_{RAKE}$  and that with a MUD receiver by  $K_{MUD}$ . We define now the efficiency  $\beta$  of MUD at a given  $E_b/N_0$  value by

$$K_{RAKE} = (1 - \beta)K_{MUD} \quad (25)$$

This applies to the macro-cell where multipath interference is significant. In a micro-cell, the channel model is close to a single path channel and thus self interference is negligible. Thus we can neglect the desired user from the total number of

users and calculate the MUD efficiency for the micro-cellular environment as

$$K_{RAKE} - 1 = (1 - \beta)(K_{MUD} - 1) \quad (26)$$

To keep the complexity of the receiver to a moderate level, we use only 4 RAKE fingers in the macro-cell with which 63 % of the total energy can be collected on the average. In the micro-cell, 95 % of the energy can be captured with 2 RAKE fingers.

We performed the link level simulations with the parameters shown in Table 1.

Table 1. Link level parameters

Chip modulation	BPSK
Data modulation	BPSK
Carrier frequency	2.0 GHz
Chip rate	5.12 Mchip/s
Spreading codes	Gold codes of length 31
Reference symbols	10 %
Coding	1/2 rate convolutional, constraint length 9
Interleaving depth	40 ms block interleaving
User data rate	74.3 kbit/s
Channel models	CODIT macro-cell, 50 km/h CODIT micro-cell, 36 km/h
Number of RAKE fingers	4 in macro-cell 2 in micro-cell
Channel estimation parameters $\gamma_1$ and $\gamma_2$	0.02
Power control	2 kHz, step size 1.0 dB, 5 % errors in feedback
Antenna diversity	2 antennas, correlation 0.7 $N_0$ is uncorrelated
Path combining method	Maximal ratio combining
Number of stages in MUD	2 (1 Interference cancelling)
Target BER	$10^{-3}$

Simulated BER curves for the micro-cell are shown in Fig. 3 and for the macro-cell in Fig. 4. All the users have equal average power. The bit error rates shown are the mean values of all the users. The single user case without intra-cell interference is shown for comparison.

included in the study to obtain the capacity for the whole network.

Table 2. Simulation results

Channel model, $E_b/N_0$ value	Number of users, no MUD, $K_{RAKE}$	Number of users with MUD, $K_{MUD}$	Efficiency of MUD $\beta$
micro, 5.1 dB	6 - 7	15	64%-71%
macro, 5.9 dB	3 - 4	10	60%-70%

The link level performance of the conventional RAKE receiver cannot be estimated assuming the interfering users from the intra-cell as Gaussian noise. First, the Gaussian approximation is not valid because we are assuming correlated antennas. The gain from antenna diversity against correlated interference is much less than against uncorrelated Gaussian noise  $N_0$ . Second, we are considering a third generation system scenario with users transmitting 74 kbit/s; therefore the system is able to support only a few users and the Gaussian approximation is valid only when a large number of users are active. In the CODIT project it was found out that when having less than 7 users with 64 kbit/s the Gaussian approximation tends to underestimate the interference [12].

For modelling the interference from the surrounding cells in the link level simulations, the Gaussian approximation is assumed to be valid as the intra-cell interference will be the dominant source of interference. Also the interference from surrounding cells originates from a larger number of mobiles compared to the intra-cell interference and thus the interference from the neighbouring cells can be modelled as additive white Gaussian noise in the link level simulations. From the analysis given in the appendix in [13], it can be seen that the difference between simulation and Gaussian approximation is very small when the number of interference sources gets large enough. Additionally the use of antenna diversity makes the interference even more Gaussian in nature. It should be noted that in the system level studies in the following chapters, the interference is always generated by the users in the network and no Gaussian approximation is used.

## 6. SYSTEM LEVEL SIMULATOR

In this section we will describe the principles used in obtaining the overall cellular system capacity. The link level simulator provides the system level simulator with required input parameters for the 74 kbit/s  $10^{-3}$  BER service under study. The link between the link level simulator and the system level simulator is presented in Fig. 5.

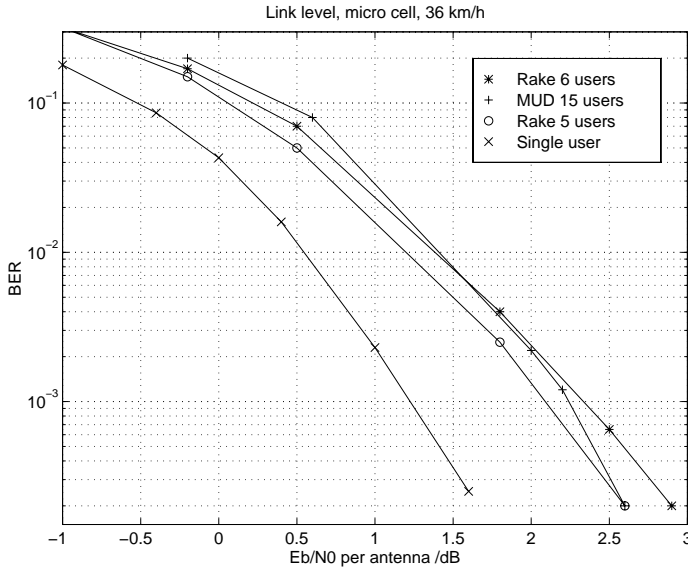


Fig. 3. BER as a function of  $E_b/N_0$  for the CODIT micro-cell

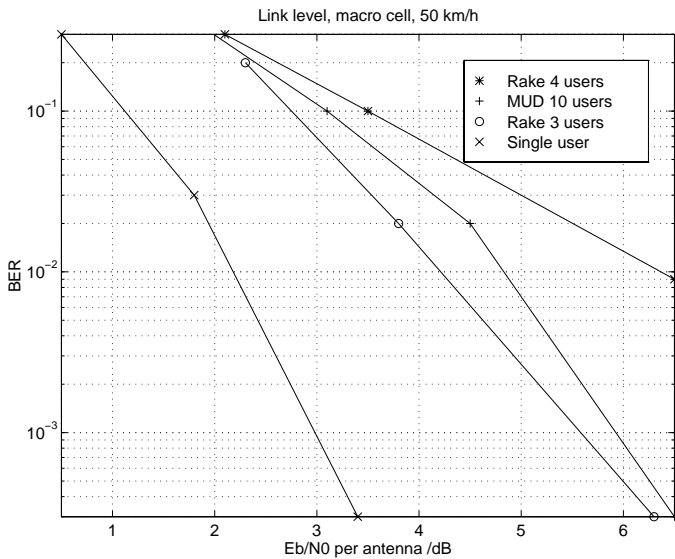


Fig. 4. BER as a function of  $E_b/N_0$  for the CODIT macro-cell

In the micro-cell we have used simulations to estimate the required  $E_b/N_0$  when 15 users are transmitting in the multiuser detection system. The capacity of the conventional RAKE receiver with the same  $E_b/N_0$  is found to be between 5 and 6 users yielding a MUD efficiency of 64 % to 71 %. In the macro-cell, the corresponding figures are 10 users with MUD and 3 to 4 users without MUD. The efficiency of MUD in macro-cell is then 60 % to 70 %. The link level simulation results and the resulting MUD efficiencies are summarised in Table 2. As the calculated MUD efficiency is valid for the intra-cell interference only, it does not directly convert to the gain in the cellular capacity. The whole network must be

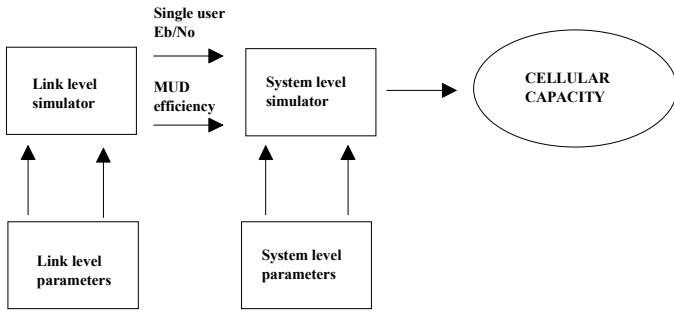


Fig. 5. The link between the link level and the system level simulator.

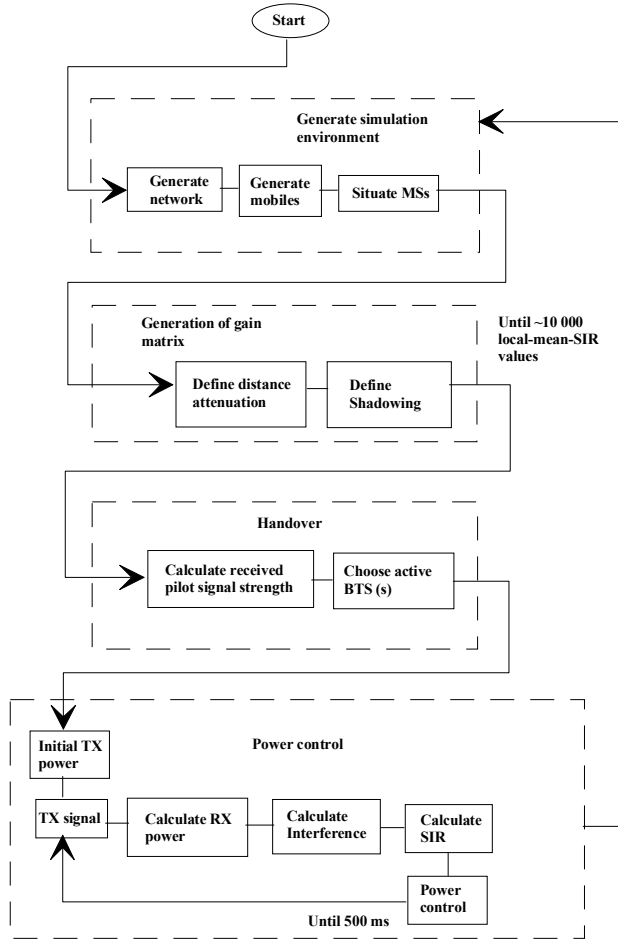


Fig. 6. The block diagram of the simulator.

The system level capacity is studied in an interference limited case and the  $E_b/(N_o+I_o)$  target is now taken as the signal to interference ratio (SIR) target. Fig. 6 presents the block diagram of the simulation algorithm. In a single simulation run, the mean SIR for each user over a 500 millisecond period is simulated. One simulation run consists of random mobile placement, virtual handover, and fast power control. We have assumed that by obtaining 10 000 local mean SIR values, uncertainty in the results is minimised. Our simulations give the outage probability for the system, where

outage probability represent the number of users having worse average SIR than required. An outage probability of 5 % was selected as the target value for capacity.

The mobile stations in the simulator are not actually moving, such as in dynamic simulators with mobility. The effect of mobility is approximated by adding a fast fading process to the signal in the system level. In this semi-static approach, mobility is a virtual procedure, but signal strength varies due to fading as a function of the mobile speed given as a parameter.

As in the link level, different simulators for micro and macro-cellular environments were used due to different propagation properties in different environments. The propagation model of the system simulator consists of attenuation, shadowing and statistically generated fast fading. Both macro and micro-cell models are adopted from [13]

In the urban macro-cell environment, the simulated network consists of 25 Base Transceiver Stations (BTS) which are located on a rectangular grid and mobiles placed randomly with a uniform distribution on the network area. The BTS positioning is presented in Fig. 7.

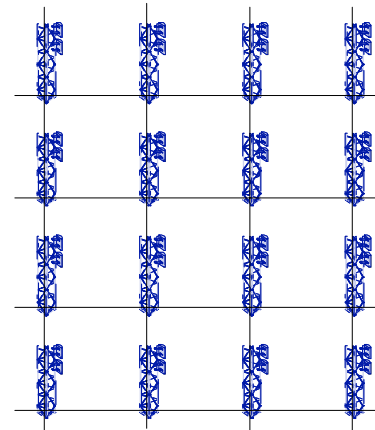


Fig. 7. Macro-cellular base station location

Shadowing is generated from a log-normal distribution with zero mean and standard deviation of 6 dB. The distance dependent attenuation is the traditional Hata model [14] converted to a frequency band around 2 GHz. The attenuation is calculated as:

$$L = 123 + 36\log(d) \quad (27)$$

In the micro-cell environment, the 32 base stations were located in every second street intersection as presented in Fig. 8. The street width used was 30 meters and the length of the building block was 100 meters. The simulated system is the so called "Manhattan grid". The shadowing is now log-normally distributed with zero mean with 4 dB standard deviation. The buildings form a heavy separation between different micro-cells. The attenuation as a function of distance was modelled with a three slopes model. Slopes are non-line-of-sight slope, and line-of-sight slope for short distances and for long

distances. If the connection between transmitter and receiver was a line-of-sight link, the attenuation is calculated as :

$$L_{LoS} = \begin{cases} 82 + 20\log\left(\frac{x}{300}\right), & \text{if } x \leq 300\text{meters} \\ 82 + 40\log\left(\frac{x}{300}\right), & \text{if } x > 300\text{meters} \end{cases} \quad (28)$$

At a distance of 300 meters, a breakpoint marks the separation between two line-of-sight segments. Turning round a corner causes an additional loss,  $L_{corner}$ , seen in (29). Attenuation between a transmitter and a receiver that have non-line-of-sight connection constitutes a line-of-sight segment, a non-line-of-sight segment, and an additional corner attenuation, as seen in (29).

$$L_{nLoS} = L_{LoS}(x_{corner}) + 17 + 0.05x_{corner} + (25 + 0.2x_{corner})\log\left(\frac{x}{x_{corner}}\right) \quad (29)$$

Line-of-sight attenuation is calculated between a corner and receiver, and non-line-of-sight connection between a corner and transmitter.

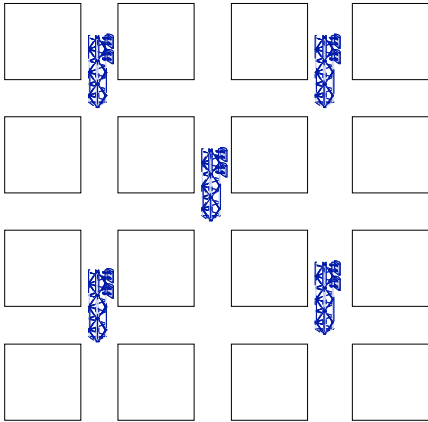


Fig. 8. The base station deployment in micro-cellular system level simulator.

The fast fading process used is produced with the algorithm presented in [10]. The fading model used is a deterministic method to simulate time correlated Rayleigh fading waveforms.

A power control algorithm is implemented as in [11]. The power control algorithm aims to keep SIR levels of users in an appropriate level by adjusting the transmission power up or down. The received SIR level is compared to the SIR threshold. If the received SIR was lower than the threshold, a power up command is sent. If the SIR level was better than the threshold a power down command is sent. Even though the system level power control is assumed error free, the fast fading process cannot be followed perfectly, and thus the capacity of the system is reduced because of imperfect power control. It should be noted that the power control command errors are modelled in the link level simulation results.

In the handover modelling, a maximum of 3 BTSs are selected in the active set. The BTSs are selected randomly with a uniform distribution from a pool of BTSs that fit in the handover margin. This non-ideal BTS selection procedure takes the effects of handovers into account. Macro-diversity (i.e. soft handover) is taken into account by selecting the best source (the frame with highest average SIR) frame-by-frame basis.

Micro-diversity (i.e. antenna diversity in the BTS) is modelled by providing four independent equal mean-strength paths in the macro-cellular environment. This corresponds the case in which there are two antennas and two RAKE receivers, both receivers with two resolvable paths. As less paths can be separated in the micro-cellular environment, only two independent equal mean-strength paths are provided. Each path fades according to a Rayleigh distributed fast fading process. The diversity combining is modelled by taking the average of the fast fading processes. It is assumed that the number of RAKE fingers is sufficient and all modelled multipath components are received. The performance loss due to the limited number of RAKE fingers, especially in the macro-cellular environment, is visible in the link level  $E_b/N_0$  values.

In the uplink when measuring SIR for a single user, the cancellation process includes all the users connected to the same BTS. It is assumed that the BTS is aware of all the users having the BTS in the active set. Interference cancellation is non-ideal with the efficiency derived from the link level simulations. Thus the total interference the BTS experiences consists of the interference from all the mobiles in the network not having a connection with the BTS and from the partly cancelled interference from the mobiles having connection to the BTS.

The effects of sectorization or other methods such as adaptive antennas to the capacity are beyond the scope of this work.

## 7. CELLULAR CAPACITIES

The uplink system level simulator was implemented using the C-language in a Unix work station. The capacity results are now presented in [users/MHz/cell]. The corresponding analytical results in [users/cell] must be divided by the channel spacing used. In Table 3 the simulation parameters are presented.

Table 3. System level parameters used.

Active set size	3
Handover margin	3 dB
Voice activity	100 %
Power control step size	1 dB
Erroneous power control commands	0 %
Micro-cell mobile speed	36 km/h
Macro-cell mobile speed	50 km/h
Channel spacing	6 MHz

In Fig. 9 the outage figures as a function of load for different MUD efficiencies for the micro-cell case are plotted. The capacity with conventional RAKE receiver is 2.0 users/MHz/cell and for the system with MUD 4.7 users/MHz/cell. The capacity is obtained with 5 % outage.

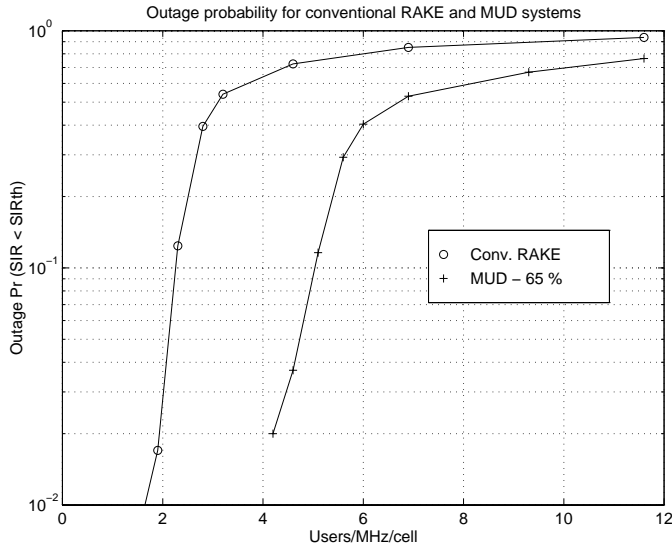


Fig. 9. Outage probability curves for micro-cells. The dashed line is the conventional case and the solid line is the MUD case with  $\beta = 60\%$ .

In Fig. 10 the simulated outage figures for the macro-cell case are presented as a function of load for different MUD efficiencies. Lines indicate performances with different MUD efficiency. From Fig. 10 it can be seen that the capacity of MUD with 65 % efficiency is almost doubled compared to the conventional RAKE receiver.

The high capacity of CDMA with MUD results from the fact that most of the interference comes from users in the same cell. Due to the soft handover, the users in a handover state can be included in the MUD process which allows an extra 20 % of interference to be included in the interference cancellation in the macro-cellular environment. In the micro-cellular environment the cell separation is better, fewer users are in the soft handover state and the amount of interference from other cells is lower than in the macro-cellular environment.

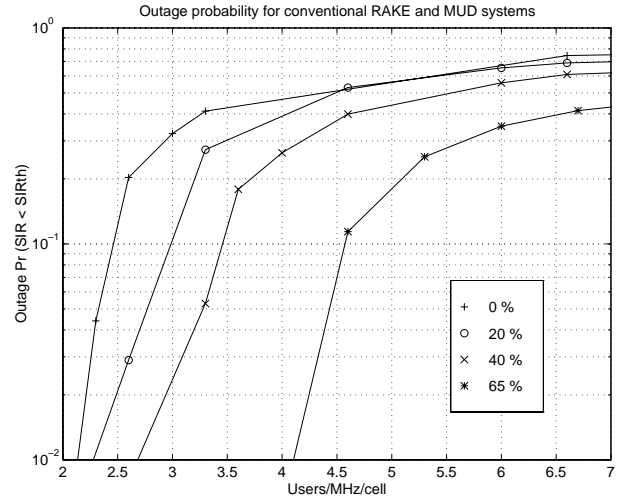


Fig. 10. Outage probability curves as a function of MUD efficiency. The line with zero percent efficiency corresponds to the conventional RAKE receiver.

To validate the simulation results, analytical capacity calculations for the macro-cellular environment were carried out. The simulated performance compared with analytical results is given in Table 4. The reason for conventional results having differences between simulated and analytical results is in the power control modelling. The analytical approach assumes perfect power control whereas the simulator has the actual power algorithm running with limited dynamics and accuracy.

Table 4. Analytical and simulated (5 % outage) capacities (users/MHz/cell).

	Conventional RAKE	MUD 20 %	MUD 40 %	MUD 65 %
Simulated	2.3	2.7	3.3	4.5
Analytical	2.8	3.3	4.0	5.3

First, the capacity formula for the network without MUD in BTS is defined. The attained  $E_b/N_0$  value is:

$$\frac{E_b}{N_0} = \frac{SG_p}{I_{intra} + I_{inter} + N_o} \quad (30)$$

where  $S$  is the received signal strength,  $G_p$  processing gain,  $I_{intra}$  intra-cell interference,  $I_{inter}$  inter-cell interference from other cells and  $N_o$  thermal noise. In the following thermal noise  $N_o$  is neglected.  $I_{intra}$  is equal to  $(N - 1)S$ .

The fraction of the intra-cell interference caused by the users operating in the same cell as the studied user compared to the total interference is given as

$$F = \frac{I_{intra}}{I_{intra} + I_{inter}} \quad (31)$$

It should be noted that in (31) the intra-cell interference  $I_{intra}$  is equal to  $NS$ , instead of  $(N - 1)S$ . The simulated value for  $F$  in macro-cells is 0.73. For a single cell  $F$  is equal to 1. From (30) and (31) we get

$$\frac{E_b}{N_0} = \frac{G_P}{\frac{N}{F} - 1} \Leftrightarrow N = F(G_P(\frac{E_b}{N_0})^{-1} + 1) \quad (32)$$

The value  $N$  is the number of users that are associated with the BTS.  $N$  also includes users that are connected to more than one BTS while in a soft handover state. The number of users being connected to two or three BTSs is obtained from the simulator and used to adjust the analysis correspondingly. The simulations show that typically in the simulated macro-cellular environment, 80 % of the users are connected to only one BTS, while 15 % of the users are connected to two BTSs and 5 % are connected to three BTSs. The calculated capacity must be then scaled by 1.25 as the effect of soft handover is seen in  $F$  and the total number of connections in the system is higher than the number of mobiles in the system.

The corresponding analysis for the MUD case can be done:

$$\frac{E_b}{N_0} = \frac{SG_P}{(1 - \beta)I_{intra} + I_{inter} + N_0} \quad (33)$$

Inter-cell interference can be calculated as:

$$I_{inter} = \frac{1 - F}{F} I_{intra} \quad (34)$$

From (33) we now get

$$\frac{E_b}{N_0} = \frac{SG_P}{(1 - \beta)(I_{intra} - S) + \frac{1 - F}{F} I_{intra}} \quad (35)$$

Since  $I_{intra}$  is equal to  $NS$ , we can write (35) now as

$$\frac{E_b}{N_0} = \frac{SG_P}{(1 - \beta)(NS - S) + \frac{1 - F}{F} NS} \quad (36)$$

The capacity of the system is now given as:

$$N = F \left( \frac{G_P(\frac{E_b}{N_0})^{-1} - (\beta - 1)}{1 - F\beta} \right) \quad (37)$$

If  $\beta$  is set to 0 in (37), then equation (37) becomes the same as (32). The  $\beta$  with value 0 represents the capacity of the conventional RAKE receiver based system.

Capacity as a function of MUD efficiency is shown in Fig. 11. Both analytical and simulated results are shown. The simulated results compare well to the analytical results. The

offset between analytical and simulated results is due the non-ideal power control.

To calibrate the simulator, an additional verification was carried out. The macro-cell performance was compared to that presented by Gilhousen et al. in [17] with the same parameters. The difference from the results in [17] was less than 10 %. The difference is mainly due to the already mentioned imperfections in the power control used. In the studied environment where a lot of diversity is achieved with wide bandwidth, an ideal power control tracking the fading perfectly could provide the ideal capacity.

It should be noted that the capacity values are valid only under the assumptions used and even then a system operating at the given capacity would be in a highly unstable state. If the interference is increased by a small amount, the system outage will drop dramatically as many users do not meet the quality criteria anymore. The power control modelling principle used results in relatively narrow C/I distribution resulting in high capacity. As the real C/I distribution is expected to be less ideal, degradation in the capacity is expected. Additionally, the performance of the backbone network in setting up new connections for soft handovers and managing the power balancing signalling in the network is also a critical factor to achieve a stable and high capacity CDMA network.

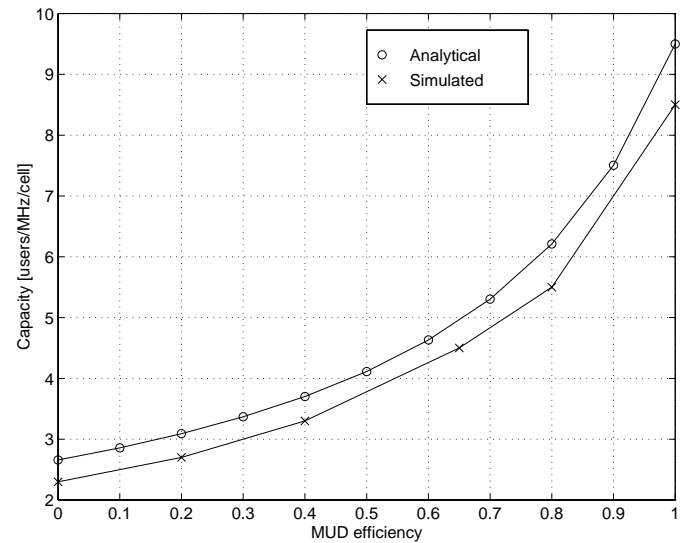


Fig. 11. Analytical and simulated capacity as a function of MUD efficiency in the macro-cellular environment.

## 8. CONCLUSIONS

The performance gain of multiuser detection over the conventional RAKE receiver has been studied by Monte Carlo simulation. The simulation models in the link level have employed antenna diversity and closed loop power control facilitating low energies per symbol. Also the link level CDMA specific features have been modelled in the system level semi-static simulator. In the macro-cell case, the number of RAKE fingers was limited and only part of the energy was captured. Still, the suboptimum multiuser receiver has been shown to offer a clearly improved link performance over the

RAKE receiver by removing 60 to 70 % of the intra-cell interference in urban micro and macro-cell environments. The CODIT macro-cell channel model allowed to collect a limited amount of energy with 4 RAKE fingers, but for channel models with less delay spread, 4 RAKE fingers will result in better energy collection in the macro-cellular environment as well. This interference reduction was used as an input to the system level simulator leading to a considerable increase in cellular capacity. The capacity gain depended on the ratio of intra-cell interference to inter-cell interference, and therefore the micro-cellular environment offering high cell isolation gained even more from the use of MUD. The alternative solutions for capacity enhancements are, for example, the use of adaptive antennas or cell splitting, which both require extra hardware like antennas etc., while with the use of MUD for capacity enhancement only baseband hardware is modified.

Multiuser detection CDMA system appears to be a promising solution for third generation mobile communication systems for both macro and micro-cellular environments by providing a considerably higher capacity than a conventional DS-CDMA RAKE receiver.

#### ACKNOWLEDGEMENTS

The authors would like to acknowledge the encouragement and the support of Dr. Jorma Lilleberg from Nokia Mobile Phones, Oulu and Dr. Kari Kalliojärvi, Mr Tero Ojanperä and Mr. Ari Hottinen from Nokia Research Center, Helsinki. The authors are also grateful for the comments given by Mr. Gerhard Kraemer from ETH Zurich and by Dr. Ian Opperman from the Center for Wireless Communications at the University of Oulu. The authors also thank the reviewers for the helpful comments given.

#### REFERENCES

- [1] M.K. Varanasi, B. Aazhang, "Multistage Detection in Asynchronous Code-Division Multiple-Access Communications", IEEE Trans. Comm., vol. COM-38, pp.509-519, April 1990.
- [2] M.K. Varanasi, B. Aazhang, "Near-Optimum Detection in Synchronous Code-Division Multiple-Access Communications", IEEE Trans. Comm., vol. COM-39, pp.725-736, April 1991.
- [3] U. Fawer, B. Aazhang, "A Multiuser Receiver for Code Division Multiple Access Communications over Multipath Channels", IEEE Trans. Comm., vol. COM-43, pp.1556-1565, February/March/April 1995.
- [4] A. Hottinen, H. Holma, A. Toskala, "Performance of Multistage Multiuser Detection in a Fading Multipath Channel", PIMRC'95 Toronto, Canada, in Proceedings, pp. 960-964, September. 1995.
- [5] A. Hottinen, H. Holma, A. Toskala, "Multiuser Detection for Multirate CDMA Communications", ICC'96, Dallas, USA, in Proceedings, pp. 1819-1823, June 1996.
- [6] Z. Zvonar, "Multiuser Detection for Rayleigh Fading Channels", Ph.D. Thesis. Northeastern University, Boston 1993.
- [7] Y.C. Yoon, R. Kohno, H. Imai, "A Spread-Spectrum Multi-Access System with a Cascade of Co-Channel Interference Cancellers for Multipath Fading Channels", ISSSTA'92 Yokohama, Japan, in Proceedings, pp. 87-90, November/December 1992.
- [8] U. Madhow, M.L. Honig, "MMSE Interference Suppression for Direct-Sequence Spread-Spectrum CDMA", IEEE Trans. Comm., vol. COM-42, pp. 3178-3188, December 1994.
- [9] R. Kohno, P.B. Rapajic, B.S. Vucetic, "An overview of Adaptive Techniques for Interference Minimization in CDMA Systems", Wireless Personal Communications, vol. 1 No 1, pp. 3-21, 1994.
- [10] RACE II, R2020 (CODIT) project, "Final Propagation Model", Deliverable to the European Commission, July 1994.
- [11] S. Verdu, "Adaptive Multiuser Detection", ISSSTA'94, Oulu, Finland, in Proceedings, pp. 43-50, July 1994.
- [12] P.G. Andermo (Ed.), RACE II, R2020 (CODIT) project, "CODIT Final Review Report", Deliverable to the European Commission, Dec. 1995.
- [13] T.S. Rappaport, "Wireless Communications - Principles and Practice", Prentice Hall, 1996.
- [14] M. Hata, "Empirical Formula for Propagation Loss in Land Mobile Radio Services", IEEE Transactions on Vehicular Technology, 29, 3, pp. 317 - 325, August 1980.
- [15] W. Jakes, "Microwave Mobile Communications", pp. 57 - 77., Wiley & Sons. 1974.
- [16] S. Ariyavisitakul, "SIR Based Power Control in a CDMA System", GLOBECOM'92, Orlando, Florida, December 1992.
- [17] K.S. Gilhousen et al. "On the Capacity of a Cellular CDMA system", IEEE Trans. Veh. Tech., vol. 40, 2, pp.303-312, May 1991.